Electron Bunch Length Measurements from Laser-Accelerated Electrons Using Single-Shot THz Time-Domain Interferometry

A. D. Debus,[1,*] M. Bussmann,[1] U. Schramm,[1] R. Sauerbrey,[1] C. D. Murphy,[2] Zs. Major,[3,4] R. Hörlein,[3,4] L. Veisz,[3] K. Schmid,[3] J. Schreiber,[3,4,5] K. Witte,[4] S. P. Jamison,[6] J. G. Gallacher,[7] D. A. Jaroszynski,[7] M. C. Kaluza,[8] B. Hidding,[9] S. Kiselev,[9] R. Heathcote,[10] P. S. Foster,[10] D. Neely,[10] E. J. Divall,[10] C. J. Hooker,[10] J. M. Smith,[10] K. Ertel,[10] A. J. Langley,[10] P. Norreys,[10] J. L. Collier,[10] and S. Karsch[3,4,*]

[1]*Forschungzentrum Dresden-Rossendorf, Institute for Radiation Physics, 01328 Dresden, Germany*
[2]*Clarendon Laboratory, University of Oxford, Parks Road, Oxford, OX1 3PU, United Kingdom*
[3]*Max-Planck-Institute für Quantenoptik, Hans-Kopfermann-Strasse 1, 85748 Garching, Germany*
[4]*Ludwig-Maximilians-Universität München, Am Coulombwall 1, 85748 Garching, Germany*
[5]*The Blackett Laboratory, Imperial College London, Prince Consort Road, London, SW7 2BW, United Kingdom*
[6]*Accelerator Science and Technology Centre, STFC Daresbury Laboratory, Warrington, WA4 4AD, United Kingdom*
[7]*University of Strathclyde, Glasgow, G4 0NG, United Kingdom*
[8]*Friedrich-Schiller-Universität Jena, Max-Wien-Platz 1, 07743 Jena, Germany*
[9]*Heinrich-Heine-Universität Düsseldorf, Universitätsstrasse 1, 40225 Düsseldorf, Germany*
[10]*Central Laser Facility, STFC Rutherford Appleton Laboratory, Chilton, Didcot, OX11 0QX, United Kingdom*

(Received 4 August 2009; published 25 February 2010)

Laser-plasma wakefield-based electron accelerators are expected to deliver ultrashort electron bunches with unprecedented peak currents. However, their actual pulse duration has never been directly measured in a single-shot experiment. We present measurements of the ultrashort duration of such electron bunches by means of THz time-domain interferometry. With data obtained using a 0.5 J, 45 fs, 800 nm laser and a ZnTe-based electro-optical setup, we demonstrate the duration of laser-accelerated, quasimonoenergetic electron bunches [best fit of 32 fs (FWHM) with a 90% upper confidence level of 38 fs] to be shorter than the drive laser pulse, but similar to the plasma period.

DOI: 10.1103/PhysRevLett.104.084802 PACS numbers: 29.25.Bx, 41.60.Dk, 52.38.Kd

Laser-plasma wakefield electron acceleration has advanced substantially over the past few years. Monoenergetic features in the electron spectra up to the GeV level, with low emittances and improved reproducibility [1–7], have been demonstrated. Laser-wakefield acceleration is a highly dynamic process as a result of a complex interplay between varying quantities such as plasma density or laser pulse energy, radius, and duration. Theory and 3D-particle-in-cell (PIC) simulations [8,9] suggest electron bunch durations inside the plasma to be inherently shorter than the plasma period λ_p/c, which for typical densities is $\simeq$10–30 fs. However, it is still not fully understood how these short pulses evolve during and after they leave the plasma, and whether their duration stays short. Previous experimental efforts [10,11] were limited in resolution to 100 fs and hence were unable to answer this question. Knowledge on post-plasma electron bunch durations is critical for compact, ultrashort x-ray sources of high brilliance such as undulator, optical wiggler or SASE free electron laser (FEL) schemes [12–17], which require electron peak currents in the kA range and pulse durations that are significantly shorter than those achieved by conventional accelerators.

We measure for the first time in a single-shot, electro-optic (EO) setup that the duration of quasimonoenergetic, laser-wakefield accelerated bunches is indeed shorter than the laser pulse duration. In the experiment, we clearly distinguish two electron distributions, accelerated by the 10 TW, 45 fs ASTRA laser pulse. We observe a long electron pulse trailing a short bunch of quasimonoenergetic electrons using coherent transition radiation (CTR) from a thin aluminum tape target following the plasma region. Knowledge of the electron energy spectrum and the geometry of the CTR source allows us to partially overcome the resolution limit of the EO crystal and infer an electron bunch duration below 38 fs (FWHM).

The experimental setup is depicted in Fig. 1. The main part of the ASTRA laser pulse (45 fs, 500 mJ) is used to accelerate electrons in a supersonic gas jet similar to that of Ref. [1]. Using transverse interferometry, the electron density is measured to be 1.5×10^{19} cm^{-3} (plasma period 30 fs). The electron spectrum is recorded using image plates and a magnetic spectrometer, while the charge is measured by an integrating current transformer (ICT).

An aluminum tape of 50 μm thickness is installed 5 mm behind the gas jet and acts as a source of coherent transition radiation (CTR), which is mainly emitted in the THz spectral range. It provides a temporal imprint of all electrons leaving the plasma and passing through the foil. In addition, the tape blocks intense THz radiation from other sources such as the plasma wakefield accelerator [18], from linear mode conversion [19], and CTR from the

© 2010 The American Physical Society

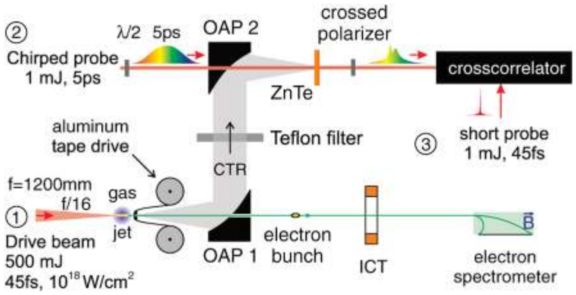

FIG. 1 (color online). Laser-accelerated electrons generate coherent transition radiation (CTR) at an aluminum tape target. The CTR is imaged by two off-axis parabolas ($f_1 = 125$ mm and $f_2 = 250$ mm) into an electro-optical ZnTe crystal, which rotates the polarization of a chirped probe (*CP*) beam in the time-domain. This modulation of the *CP* is analyzed in a cross correlator.

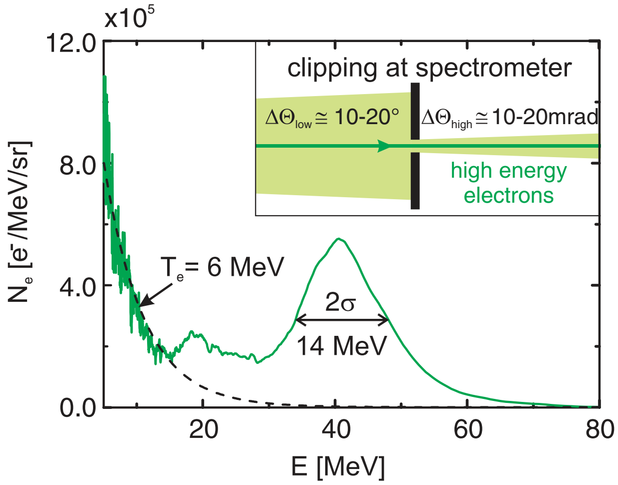

FIG. 2 (color online). A typical electron spectrum as recorded with the pulse duration measurement. Because of clipping at the spectrometer aperture, the number of low-energy electrons (dashed line) reaching the spectrometer is reduced by more than an order of magnitude.

plasma-vacuum transition [10]. The CTR emitted from the tape is collimated and focused into a 200 μm thick ZnTe crystal ($\langle 110 \rangle$ orientation, supplied by Ingcrys laser systems) using a pair of off-axis parabolas (OAPs), the first of which is equipped with a central hole (1 cm dia.) to transmit the electrons and the drive laser beam. A Teflon filter placed between the OAPs additionally blocks scattered laser light. From the ASTRA pulse, 1 mJ is split off, negatively chirped to 5 ps duration in a Treacy-type grating arrangement and focused through the ZnTe crystal. The EO crystal material was chosen for its high nonlinear coefficient and the thickness of 200 μm to minimize signal-probe group velocity walk off. Because the diffraction limited beam ($w_0 = 100$ μm) is offset by $d = 600$ μm from the radially polarized CTR focus, the THz field polarization within the probe beam can be assumed to be linear. The transient birefringence induced in the crystal by the THz pulse via the electro-optic Pockels effect rotates the polarization of the chirped probe (*CP*) beam. The resulting change in polarization encodes an intensity modulation onto the *CP* after passing through a crossed polarizer. The temporal evolution of this intensity modulation—and thus the temporal structure of the CTR pulse—is then probed directly by another 1 mJ, 45 fs part of the ASTRA laser pulse in a cross correlator, similar to that in [20,21].

For the analysis of the experimental data, we assume the electron beam to consist of a low-emittance ultrashort electron bunch followed, after a time $\Delta\tau$, by a divergent tail of low-energy electrons with a temperature T_e and duration τ_{long}. This assumption is motivated by simulations of the highly nonlinear broken-wave regime [8], and it is experimentally supported by simultaneously recorded electron spectra, such as the one shown in Fig. 2. The spectrum suggests that one part of the 30 pC electron beam is accelerated to an energy of 40 MeV, with an rms energy spread of 7 MeV, while the rest of the beam, the low-energy part, exhibits an exponential spectrum with $T_e = 6$ MeV. The existence of two temporally separated electron populations is confirmed by the doubly peaked cross-correlator intensity trace as shown in Fig. 3(b)(2) and was only measured when monoenergetic features were present in the electron spectrum.

The ZnTe crystal has a transverse optical phonon resonance at 5.3 THz, which limits the intrinsic resolution to $\simeq 180$ fs. To understand how to overcome this limit, consider a Gaussian-type CTR pulse much shorter than the temporal resolution limit. In the spectral domain, this is equivalent to a Gaussian spectrum centered around zero frequency [22–24], which reaches far beyond the observable ZnTe frequency window. Inside that window, it displays a nearly constant spectral amplitude. However, different pulse durations can still be differentiated by their spectral amplitude at the cutoff frequency. Thus, the ratio of the spectral energy at high frequencies and the total radiated energy are a sensitive indicator of electron bunch duration variations. To detect them, we make use of the sharp, threefold increase in the ZnTe index of refraction between 4 and 5 THz close to the resonance. This increase delays and attenuates the high-frequency components, which in the time domain appear as damped field oscillations trailing the main pulse as in the blue curve in Fig. 3(b)(1).

If the ultrashort THz signal would be fully transmitted, one could hardly distinguish these oscillations from the background electrons. We have thus enhanced the mutual contrast of the THz signals from the long and short electron bunch by using the central hole in the parabola as an angular filter, thereby selectively reducing the intensity of the reflected ultrashort THz fields from the high electron energy contribution ($\theta \simeq 1/\gamma$). The idea behind our analysis is a time-domain interferometry (TDI) approach to separate the superposed signal from our measurement into its constituent CTR fields by distinguishing the differ-

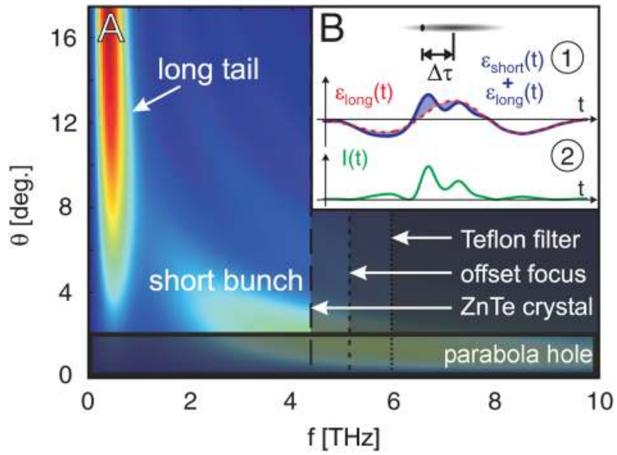

FIG. 3 (color). (a) The angular-spectral intensity of coherent transition radiation (CTR) from a short electron bunch ($\tau_{\text{short}} = 32$ fs) followed after a time $\Delta\tau = 356$ fs by a long, low-energy electron background ($\tau_{\text{long}} = 712$ fs) is constrained by several filter functions (arrows illustrate respective cutoff frequencies), affecting the overall time resolution. (b) In the time domain, the CTR field is a superposition of the low-energy electrons (red curve) trailing in the wake of an ultrashort, subresolution electron bunch (1). The resulting interference (green curve) is measured as an intensity trace in the cross correlator and includes effects of polarization optics (2).

ent time scales. Hence, we have a long, above-resolution background field $\varepsilon_{\text{long}}(t)$ [red curve in Fig. 3(b)(1)], which is easy to characterize and a short, subresolution field of the ultrashort electron bunch $\varepsilon_{\text{short}}(t)$ that now modifies a known background.

By using the long background field $\varepsilon_{\text{long}}(t) > \varepsilon_{\text{short}}(t)$ as a bias for the electric field $\varepsilon_{\text{short}}(t)$, this background defines a zero-field reference for the short THz field and thus preserves the latter's sign information in the cross-correlator intensity trace $I(t)$ [see green curve in Fig. 3(b)(2)]. For the same reason, the measurement is also robust against small polarization imperfections within the diagnostic system, which affect the entire signal, but not the field amplitudes of the short pulse with respect to the reference background.

The measured electron spectra allow calculation of the CTR radiation angles ($\theta \propto 1/\gamma$). This gives the fraction of the CTR spectrum that is transmitted by the OAPs to the ZnTe crystal. Using the ZnTe crystal properties from Ref. [25], we model the EO crystal response according to Ref. [22]. The resulting oscillations of the high-frequency components are then compared with the measured cross-correlator signal and enable the deduction of the original ultrashort bunch durations well below 100 fs (FWHM).

For the detailed modeling of the transition radiation of the electrons after the Al foil, we take into account diffraction effects [24] because the closely spaced tape holders behind the foil define a finite emission region with an effective size of 2 mm. If electron spectra were measured for a given shot, they were taken as the basis for the modeling of the long and short electron distributions and divided into an exponential, low-energy part and a quasi-monoenergetic feature at higher energies. The simulated far-field distribution was propagated using Fourier optic techniques through a model of the THz refocusing optics, including the holes in the OAPs. For the focusing, we take into account the full radially polarized THz beam and the 100 μm diameter *CP* focus, which is displaced by 600 μm from the THz pulse axis. This offset introduces another high-frequency cutoff, since high frequencies are focused to a spot too tight to interact with the off-center *CP* beam. The result is a spatiotemporal field distribution at the focus in the ZnTe crystal. In the next modeling step, we track the THz pulse and the *CP* through the crystal [22,23]. The transmission of the *CP* through the crossed polarizer, carrying the temporal information, is modeled using the Jones matrix formalism. The final optical pulse intensity measured by the cross correlator is given by the square of the *CP* electric field.

The measured cross-correlator intensity trace (black curve in Fig. 4) of the sample shot from Fig. 2 is fitted to the model with the main parameters being τ_{short}, τ_{long}, $\Delta\tau$, and the number ratio η_{el} of the two electron populations.

We calculate the influence of shot-to-shot fluctuations, characterized in 19 calibrations measurements, on our fitting parameters using a Monte Carlo approach. First, a range of synthetic data sets is generated by adding statistical noise, equivalent to the measured shot-to-shot fluctuation, to the best fit (based on minimum χ^2). Then, these data sets are used as input for our fitting algorithm, which results in distributions of fitting parameters [see Fig. 4(b)–4(d)], where each fit is marked by a blue dot.

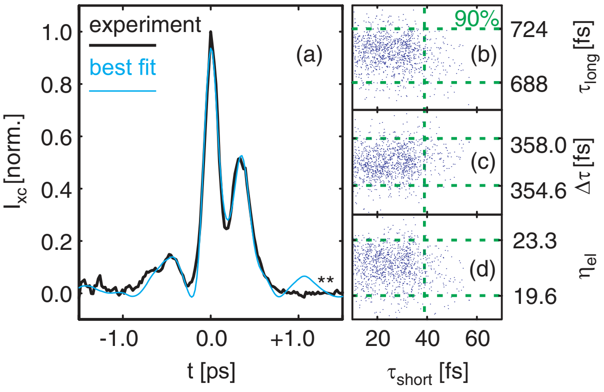

FIG. 4 (color online). (a) The model of two electron distributions is fitted to the measured cross-correlator intensity trace determining the short pulse duration with a best fit at $\tau_{\text{short}} = 32$ fs (FWHM), the temporal offset $\Delta\tau = 356$ fs, and the long electron background duration $\tau_{\text{long}} = 712$ fs (FWHM). (b)–(d) depicts error margins at the 90% level of τ_{short}, τ_{long}, $\Delta\tau$, and η_{el}. The dots represent fits to random variations of the best fit ($**$). This deviation is consistent with a non-Gaussian, low-energy tail at later times, which does not affect the short pulse duration measurement.

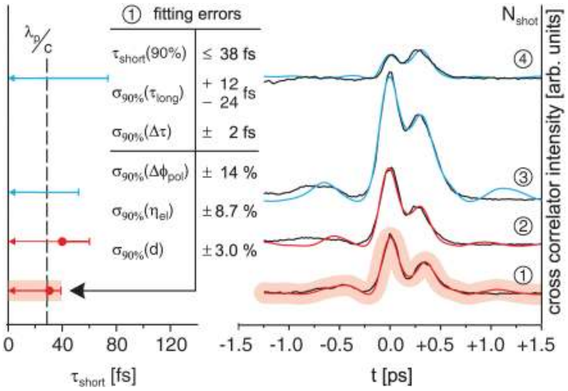

FIG. 5 (color). Left: Bunch duration measurements of several shots including all error contributions. Right: Corresponding measured cross-correlator traces (black) with best fits (colored). For the calculation of the red curves, a measured electron spectrum was available. The best fit electron bunch duration of shot no. 1 (highlighted) is 32 fs and thus comparable to the measured plasma period $\lambda_p/c = 30$ fs (dashed line).

For the shot in Fig. 4, we determined a best fit at $\tau_{\text{short}} = 32$ fs (FWHM) with 90% of all Monte Carlo scenarios below 38 fs (FWHM). Figures 4(b)–4(d) illustrate error margins of $\tau_{\text{long}} = 712^{+12}_{-24}$ fs and $\Delta\tau = 356^{+1.5}_{-1.8}$ fs. The relative uncertainties due to the small misalignment in polarization optics $\Delta\phi_{\text{pol}}$, the electron number ratio η_{el}, and the CP to CTR offset d are 14.0%, 8.7%, and 3.0%, respectively.

Typical background electron durations τ_{long} from various shots were determined to be in a range of 450–800 fs with delays $\Delta\tau$ of 300–450 fs behind the respective ultrashort electron bunches. These delays and bunch durations are in good agreement with the time-of-flight dispersion of the low-energy electrons as they propagate over a distance of 5 mm to the Al foil. A selected set of four shots with corresponding short electron bunch durations and the respective fits is displayed in Fig. 5. For shots (1) and (2) (red lines), electron spectra could be used for detailed modeling [24]. Although the electron spectrometer was not in operation for shots (3) and (4) (blue lines), considerable information can be retrieved based on spectra comparable to (1) and (2) combined with assuming varying energies of their monoenergetic peaks. However, due to this uncertainty in shot (3) and (4), no best fit could be obtained for the short bunch duration τ_{short}. Shot (1), corresponding to Fig. 4, has a 90% upper limit at 38 fs and a best fit at 32 fs, which suggests an electron bunch duration comparable to or shorter than the plasma period $\lambda_p/c = 30$ fs. While the best fit value is slightly above the pulse duration expected by PIC simulations [9], it has to be pointed out that no lower limit can be given and that effects such as beam loading [26] can lead to a substantial elongation with respect to ideal case PIC scenarios with durations well below half the plasma period.

In summary, we presented first experimental results that laser-plasma wakefield accelerated electrons are in fact shorter than the drive laser pulse duration, even after exiting the plasma. We found an upper limit of 38 fs (FWHM) on the electron bunch duration at a laser pulse duration of 45 fs, showing it to be comparable to the plasma period. This paves the way towards future ultrashort x-ray sources of high brilliance, such as ultrafast Thomson-scattering [14,15] or, in a more long-term perspective, a laboratory-scaled SASE FEL [16], for which ultrashort electron pulses with high peak currents in the kA range are essential. These developments might make compact, brilliant x-ray beams for applications available in midsized university labs.

This work was also supported by the EU Access Grant No. R113-CT-2003-506350 of the Central Laser Facility (CLF) at Rutherford Appleton Laboratory, UK, the Research Councils, UK, and the ALPHA-X project.

---

*a.debus@fzd.de and stefan.karsch@mpq.mpg.de

[1] S. P. D. Mangles *et al.*, Nature (London) **431**, 535 (2004).
[2] C. G. R. Geddes *et al.*, Nature (London) **431**, 538 (2004).
[3] J. Faure *et al.*, Nature (London) **431**, 541 (2004).
[4] W. P. Leemans *et al.*, Nature Phys. **2**, 696 (2006).
[5] R. P. Shanks *et al.*, Proc. SPIE Int. Soc. Opt. Eng. **7359**, 735907 (2009).
[6] J. Osterhoff *et al.*, Phys. Rev. Lett. **101**, 085002 (2008).
[7] S. Karsch *et al.*, New J. Phys. **9**, 415 (2007).
[8] A. Pukhov and J. Meyer-ter Vehn, Appl. Phys. B **74**, 355 (2002).
[9] M. Geissler, J. Schreiber, and J. Meyer-ter Vehn, New J. Phys. **8**, 186 (2006).
[10] J. van Tilborg *et al.*, Phys. Rev. Lett. **96**, 014801 (2006).
[11] T. Ohkubo *et al.*, Phys. Rev. ST Accel. Beams **10**, 031301 (2007).
[12] H.-P. Schlenvoigt *et al.*, Nature Phys. **4**, 130 (2008).
[13] M. Fuchs *et al.*, Nature Phys. (to be published).
[14] A. D. Debus *et al.*, Proc. SPIE Int. Soc. Opt. Eng. **7359**, 735908 (2009).
[15] H. Schwoerer, B. Liesfeld, H. P. Schlenvoigt, K. U. Amthor, and R. Sauerbrey, Phys. Rev. Lett. **96**, 014802 (2006).
[16] F. Grüner *et al.*, Appl. Phys. B **86**, 431 (2007).
[17] D. A. Jaroszynski *et al.*, Phil. Trans. R. Soc. A **364**, 689 (2006).
[18] R. A. Bosch, Phys. Plasmas **13**, 113107 (2006).
[19] H. C. Wu, Z. M. Sheng, Q. L. Dong, H. Xu, and J. Zhang, Phys. Rev. E **75**, 016407 (2007).
[20] S. P. Jamison *et al.*, Opt. Lett. **28**, 1710 (2003).
[21] G. Berden *et al.*, Phys. Rev. Lett. **93**, 114802 (2004).
[22] S. Casalbuoni *et al.*, Phys. Rev. ST Accel. Beams **11**, 072802 (2008).
[23] S. Casalbuoni *et al.*, DESY Hamburg Tech. Report No. 2005-01, 2005.
[24] J. van Tilborg *et al.*, Laser Part. Beams **22**, 415 (2004).
[25] G. Gallot *et al.*, Appl. Phys. Lett. **74**, 3450 (1999).
[26] M. Tzoufras *et al.*, Phys. Rev. Lett. **101**, 145002 (2008).